

Suspended carbon nanotube quantum dots with two gates

Jien Cao, Qian Wang, Dunwei Wang and Hongjie Dai ^{a)}

Department of Chemistry and Laboratory for Advanced Materials, Stanford University,
Stanford, CA 94305

Suspended single-walled carbon nanotube devices comprised of high quality electrical contacts and two electrostatic gates per device are obtained. Compared to nanotubes pinned on substrates, the suspended devices exhibit little hysteresis related to environmental factors and manifest as cleaner quantum resonators or single electron transistors. The high-field saturation currents in suspended nanotubes related to optical phonon or zone boundary phonon scattering are significantly lower due to the lack of efficient heat sinking. The multiple gate design may facilitate the investigation of electromechanical properties of nanotube quantum systems.

^{a)} Electronic mail: hdai@stanford.edu

In recent years, successful fabrication of suspended single-walled carbon nanotube (SWNT) devices with electrical wiring has facilitated the investigation of the electrical, mechanical and electromechanical properties of these novel wires.¹⁻⁶ Here, we report a reliable method for the fabrication of suspended SWNT devices with improved metal-nanotube contacts and a useful double-gate design. These devices have led to the revelation of interesting electrical transport properties of nanotubes that are distinct from those pinned on substrates.

The structure of our suspended SWNT device is shown in Fig. 1, consisting of a nanotube suspended over a trench by two pre-formed source (S) and drain (D) metal electrodes, a metal local-gate (V_{GL}) at the bottom of the trench and a global Si back-gate (V_{GB}). Device fabrication started with deposition of a 38 nm thick Si_3N_4 film on a p-type SiO_2/Si wafer (SiO_2 thickness = 500 nm). Electron-beam lithography (EBL) was used to define the local-gate pattern, dry-etching and wet-etching were used to open a window in the EBL resist and Si_3N_4 film and to further etch ~300 nm deep into the SiO_2 to form a trench with undercut (Fig. 1a). Electron beam deposition of Pt/W (25 nm Pt; 5 nm W as sticking layer) followed by lift-off was then carried out to complete the formation of the trench with a Pt/W local gate electrode at the bottom. A second step EBL was performed to define the S/D pattern, followed by deposition of 5 nm W (as the sticking layer) and 25 nm Pt, and then liftoff. The region across the trench was written into a continuous stripe in this EBL step. After metal deposition and liftoff, the stripe gave rise to the S/D electrodes separated by the trench. The S/D extended to the two edges of the trench and were electrically isolated from the local Pt gate due to undercutting in the sidewall of the

trench. Finally, a third EBL step was carried out to pattern catalyst islands on top of the S/D. Chemical vapor deposition (CVD) was then used to grow SWNTs to bridge the electrode pairs on the wafer chip.^{4,5} Low yield growth conditions were used (800 – 825 °C) to afford mostly single tubes bridging the S/D pairs, as confirmed by scanning electron microscope (SEM) after electrical measurements of the devices. The results presented here were all obtained from individual suspended SWNT devices.

Earlier, we described CVD growth of SWNTs across pre-formed Mo electrodes for electrical and electromechanical devices.⁴ Mo was chosen as the S/D electrode material due to its compatibility with SWNT growth. In the current work, we succeeded in using W or Pt/W as preformed electrodes and found that the typical resistance of our individual suspended SWNT devices was in the range of 10 – 50 kΩ (Fig. 2 to 4). The contact resistance was lower than those with Mo electrodes but higher than our recent devices with nanotubes lying on substrates with Pd top-contacts.⁷

We observed several interesting properties for suspended SWNTs that were distinct from nanotubes pinned on substrates. The first was that the suspended devices exhibited no hysteresis in current vs. gate (I_{sd} - V_{GL}) sweeps when placed in Ar, dry air or vacuum (Fig. 2a inset). This differed from nanotubes resting on SiO₂ substrates and was attributed to the lack of water molecules adsorbed on nanotubes in a dry environment, and that suspended nanotubes were free from intimate contact with water molecules adsorbed on SiO₂ substrate.⁸

The second interesting property of the suspended nanotube devices was that they appear to be ‘cleaner’ quantum systems than nanotubes on substrates. At low temperatures, the devices (length of suspension investigated here $L \sim 400$ -700 nm)

exhibited characteristics corresponding to single quantum dots or interference resonators, without complex dots-in-series behavior often observed for tubes on substrates. A representative small band-gap semiconducting (SGS) SWNT⁹ device is shown in Fig.2. The temperature dependence of the dip in the I_{sd} - V_{GL} in Fig. 2a shows activated transport. A small band gap of $E_g \sim 70$ meV is obtained by fitting the conductance (G) at the dip to $\exp(-E_g/2K_B T)$. Transport through the p- and n-channels of the SWNT appear asymmetric, with higher conductance for the p-channel. At T=100 K, the subthreshold swings are $S \sim 150$ mV/decade and 1.2 V/decade for the p- and n-channels respectively.

At this temperature, the expected¹⁰ S is $S = \frac{1}{\alpha_{GL}} \cdot \frac{kT}{e} \ln 10 \approx 130$ mV/decade, where $\alpha_{GL} \sim 0.15$ is the local-gate efficiency factor (shift in Fermi level for a gate voltage change of $\Delta V_{GL} = 1$ V) as deduced later. Comparison of p- and n-channels' subthreshold swings to the expected value suggests near zero and appreciable positive Schottky Barriers (SBs)^{7,11} to the valence and conduction bands respectively between the SGS tube and the S/D electrodes.

A lock-in technique (503 Hz, 50 μ V S/D bias) was used to perform dI_{sd}/dV_{sd} measurements for the p-channel of our suspended-SWNT devices. When the local gate was set at a constant of $V_{GL} = -3.0$ V, dI_{sd}/dV_{sd} vs. V_{GB} and V_{sd} exhibits an interference pattern with conductance peaks ($\sim 45 \mu$ S, $1.4e^2/h$) and valleys ($\sim 15 \mu$ S, $0.5e^2/h$) (Fig.2b). The conductance peaks at $V_{sd} \sim 2.8$ mV corresponds to the length of the nanotube $L \sim 620$ nm very well through $V_c = h v_F / 2L \sim 1.67$ meV/L(μ m), suggesting that the p-channel of the SGS tube behaves as a well-defined interference wave guide or resonator.¹²⁻¹⁴

The n-channel of the device exhibits clear Coulomb blockade (CB) behavior (Fig. 2c), as probed by fixing $V_{GL} = 3.5$ V and sweeping V_{GB} . The SBs to the conduction band

give rises to two contact barriers that confine the nanotube quantum dot (QD). Clean periodic CB features corresponding to a single QD were observed with a charging energy of $E_c \sim 13$ meV. Since the length of the nanotube is $L = 620$ nm, a charging energy of ~ 13 meV appears higher than $E_c \sim 5$ meV/ $L(\mu\text{m}) \sim 8$ meV typically expected¹⁵ for nanotubes QDs on SiO₂ substrates. This discrepancy is likely to be due to the low dielectric constant of the medium (air/vacuum) surrounding the suspended nanotube (compared to SiO₂ for tubes on substrate), which gives rise to a lower total capacitance and thus higher charging energy for the suspended nanotube. A modified relation of $E_c \sim 8$ meV/ $L(\mu\text{m})$ is able to fit the charging energies of our suspended nanotubes well. The local-gate efficiency is estimated to be $\alpha_{GL} = E_c/\Delta V_{GL} = 0.15$ where $\Delta V_{GL} \sim 87$ mV is the period of Coulomb oscillation in Fig. 2c. We also observed extra lines outside the CB diamonds (Fig. 2c inset), corresponding to excited quantum confined states along the length of the tube. The energy scale of the lines is ~ 2 meV, matching the discrete level spacing¹⁵ of $\Delta E \sim 1$ meV/ $L(\mu\text{m})$ in the nanotube.

We note that clean and homogeneous quantum resonators or dots are reliably observed with large numbers of our suspended-SWNT devices, at much higher frequency than tubes on substrates with similar lengths between S/D electrodes as the suspended ones. This suggests few defects in our SWNTs at the sub-micron length scale and the lack of substrate-nanotube interactions can prevent the break up of nanotubes into segments due to local chemical effects or mechanical strains.

A third interesting feature of our suspended nanotube devices is the two-gate configuration. We have measured the conductance of the sample versus both gates, as shown in Fig. 3. The slopes of the bright lines in G vs. V_{GL} and V_{GB} can be used to

deduce the ratio between the efficiencies of the two gates, $\alpha_{GL}/\alpha_{GB} \sim 30$. That is, the local-gate is ~ 30 times more efficient than the back-gate, or the local gate capacitance $C_{GL} \sim 30C_{GB}$. The low efficiency of the back-gate can be understood due to screening of the local gate (Fig. 1). Note that the local gate capacitance can be predicted by¹⁶

$$C_{GL} \approx \frac{2\pi\epsilon\epsilon_0 L}{\ln(2h/r)} \approx 5 \times 10^{-18} F, \text{ where } \epsilon = 1, r \sim 1 \text{ nm is the nanotube radius and } h = 300 \text{ nm}$$

is the distance between the local gate and the nanotube (depth of trench). This suggests that $C_{GB} \sim C_{GL}/30 \sim 1.7 \times 10^{-19} F$, which is in reasonable agreement with $C_{GB} \sim 0.9 \times 10^{-19} F$ as measured from the CB data in the inset of Fig. 2c. A potentially powerful aspect of the two-gate configuration is that under appropriate conditions, the local gate electrostatic coupling could become sufficiently strong to induce appreciable mechanical strain in the nanotube. The less effective global back-gate could then be used as a sweeping gate to characterize the electromechanical effects to the suspended nanotube quantum dot. We are currently pursuing this interesting possibility, especially for electromechanical measurements at low temperatures.

The fourth interesting result obtained with our suspended SWNT devices concerns about the high field transport properties of nanotubes when they are not resting on underlying substrates. This can shed light into the properties of nanotubes in their intrinsic states without significant roles played by the environment. For all of the suspended nanotubes that we have measured ($L \sim 400 - 700$ nm, resistance $\sim 40 - 60$ k Ω), we have consistently observed current saturation at the $I_{sat} \sim 8 \mu\text{A}$ level, which is significantly lower than $\sim 15-20 \mu\text{A}$ saturation currents for nanotubes (with similar resistance) lying on substrates. Since current saturation at high fields in SWNTs is

caused by scattering of energetic (~ 0.2 eV) optical or zone-boundary phonons,¹⁷⁻¹⁹ the lower saturation current in a suspended nanotube can be understood by the lack of a proximal thermally conductive SiO_2 substrate for ‘heat sinking’. Electrical heating is rapid in suspended nanotubes and the heat cannot be efficiently conducted away to the surrounding. With heating and the presence of excited phonon modes that cannot be rapidly dissipated, electron scattering appears more efficient in suspended nanotubes as reflected by the low saturation currents.

In summary, a reliable method has been developed to obtain suspended SWNT devices with relatively good electrical contacts. Compared to nanotubes lying on substrates, the suspended devices exhibit little hysteresis behavior and manifest as well-defined single quantum dots or resonators. The high field saturation current caused by optical phonon scattering in suspended nanotubes is low. The multiple gate design may facilitate the investigation of electromechanical properties of nanotubes.

This work was supported by a NSF-NIRT grant, a Packard Fellowship, Sloan Research Fellowship and a Camille Dreyfus Teacher-Scholar Award.

Figure Captions:

Figure 1. (a) A schematic device structure. (b) SEM images of a device consisting of a single suspended nanotube.

Figure 2. (a) I_{sd} - V_{GL} characteristics for a suspended SWNT device (with back-gate grounded) recorded from room temperature to 1.5 K (curve with drastic oscillations). Inset: Hysteresis free double-sweep I_{sd} - V_{GL} data recorded at room temperature. (b) A zoom in of (a) in a smaller gate range V_{GL} of 2 - 5V. Inset: A 2-D plot of dI_{sd}/dV_{sd} vs. V_{GB} and V_{sd} (V_{GL} set at 3.5 V). (c) A 2-D plot of dI_{sd}/dV_{sd} vs. V_{GB} and V_{sd} (V_{GL} fixed at -3.0V).

Figure 3. A 2-D plot of current vs. V_{GL} and V_{GB} under $V_{sd} = 1$ mV. The bright color corresponds to high conductance of $1.4 e^2/h$ and dark color corresponds to zero conductance.

Figure 4. I_{sd} - V_{sd} curve recorded for a suspended SWNT up to a high bias of $V_{sd} = 2$ V.

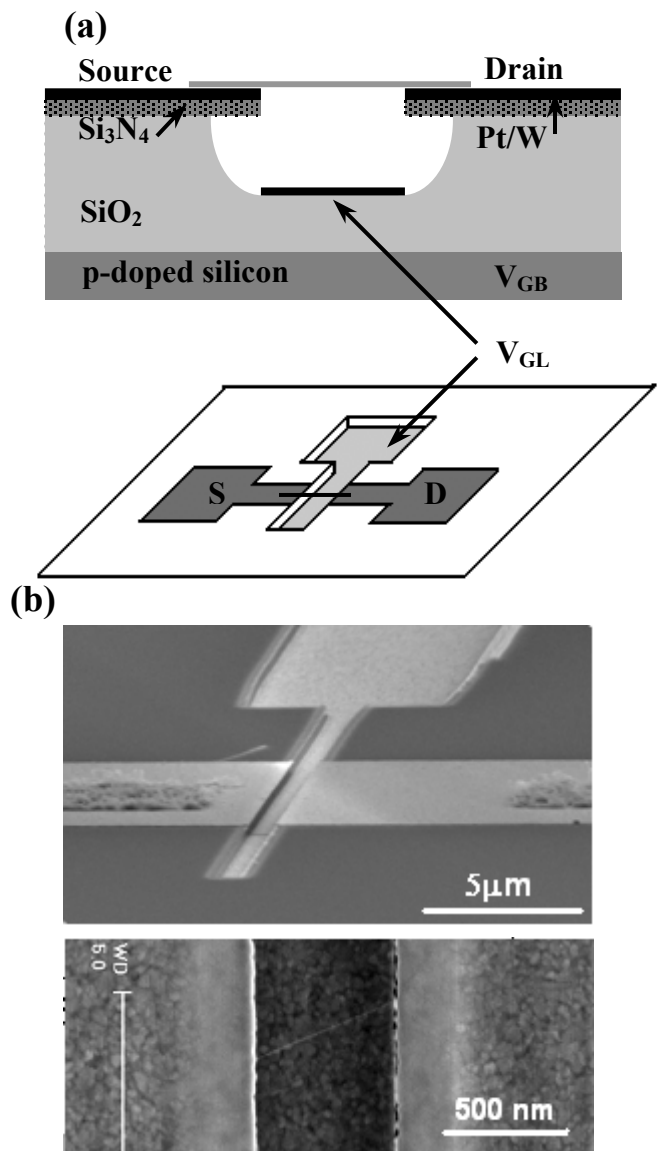


Figure 1

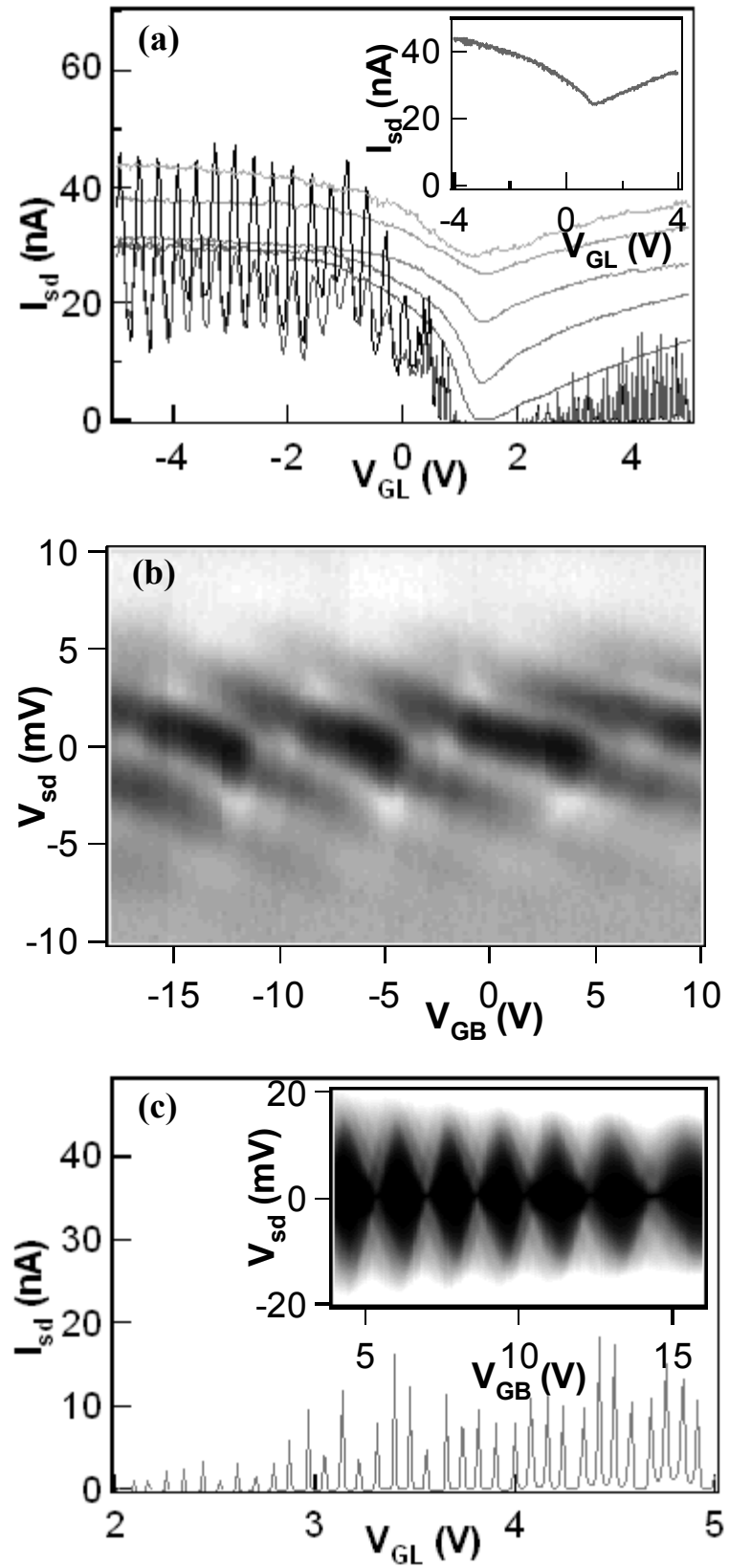


Figure 2

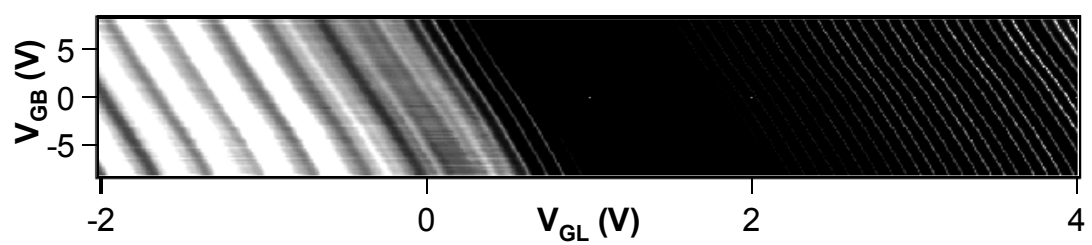


Figure 3

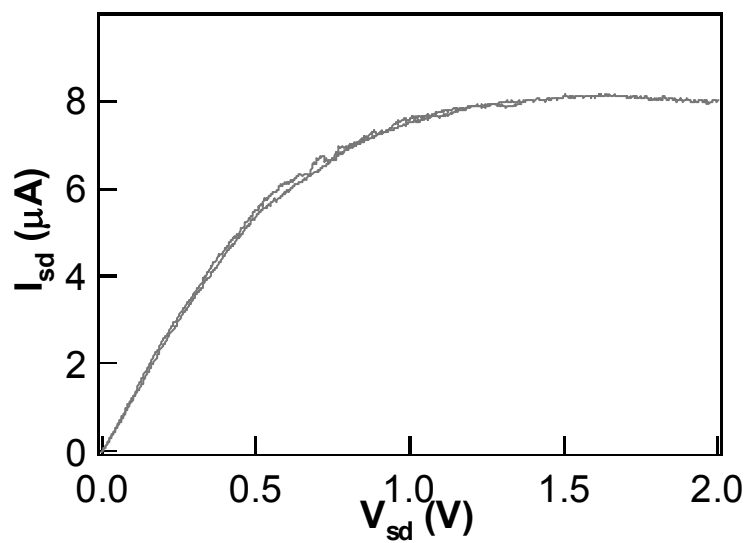


Figure 4

References

- ¹ T. Tombler, C. Zhou, L. Alexeyev, et al., *Nature* **405**, 769 (2000).
- ² D. Walters, L. Ericson, M. Casavant, et al., *Appl. Phys. Lett.* **74**, 3803 (1999).
- ³ J. Nygard and D. Cobden, *Appl. Phys. Lett.* **79**, 4216 (2001).
- ⁴ N. R. Franklin, Q. Wang, T. W. Tombler, et al., *Appl. Phys. Lett.* **81**, 913 (2002).
- ⁵ J. Cao, Q. Wang, and H. J. Dai, *Phys. Rev. Lett.* **90**, 157601 (2003).
- ⁶ E. D. Minot, Y. Yaish, V. Sazonova, et al., *Phys. Rev. Lett.* **90**, 156401 (2003).
- ⁷ A. Javey, J. Guo, Q. Wang, et al., *Nature* **424**, 654 (2003).
- ⁸ W. Kim, A. Javey, O. Vermesh, et al., *Nano Lett.* **3**, 193 (2003).
- ⁹ C. Zhou, J. Kong, and H. Dai, *Phys. Rev. Lett.* **84**, 5604 (2000).
- ¹⁰ S. M. Sze, *Physics of semiconductor devices* (Wiley, New York, 1981).
- ¹¹ S. Heinze, J. Tersoff, R. Martel, et al., *Phys. Rev. Lett.* **89**, 6801 (2002).
- ¹² W. Liang, M. Bockrath, D. Bozovic, et al., *Nature* **411**, 665 (2001).
- ¹³ J. Kong, E. Yenilmez, T. W. Tombler, et al., *Phys. Rev. Lett.* **87**, 106801 (2001).
- ¹⁴ D. Mann, A. Javey, J. Kong, et al., *Nano Lett.* **3**, 1541 (2003).
- ¹⁵ J. Nygard, D. H. Cobden, M. Bockrath, et al., *Appl Phys A* **69**, 297 (1999).
- ¹⁶ S. Ramo, J. R. Whinnery, and T. V. Duzer, *Fields and Waves in Communication Electronics* (Wiley, New York, 1994).
- ¹⁷ Z. Yao, C. L. Kane, and C. Dekker, *Phys. Rev. Lett.* **84**, 2941 (2000).
- ¹⁸ A. Javey, J. Guo, M. Paulsson, et al., cond-mat/0309242.
- ¹⁹ J.-Y. Park, S. Rosenblatt, Y. Yaish, et al., cond-mat/0309641.